Journal of Quantitative Spectroscopy & Radiative Transfer 129 (2013) 199–203

Contents lists available at ScienceDirect

Journal of Quantitative Spectroscopy & Radiative Transfer

journal homepage: www.elsevier.com/locate/jqsrt

Efficient computation of some speed-dependent isolated line profiles

H. Tran *, N.H. Ngo, J.-M. Hartmann

Laboratoire Interuniversitaire des Systèmes Atmosphériques, UMR CNRS 7583, Université Paris Est Créteil, Université Paris Diderot, Institut Pierre-Simon Laplace, 94010 Créteil Cedex, France

ARTICLE INFO

Article history:
Received 16 April 2013
Received in revised form
13 June 2013
Accepted 14 June 2013
Available online 21 June 2013

Keywords:
Line-shape
Speed-dependent profiles
Complex probability function

ABSTRACT

This paper provides FORTRAN subroutines for the calculation of the partially-Correlated quadratic-Speed-Dependent Hard-Collision (pCqSDHC) profile and of its two limits: the quadratic-Speed-Dependent Voigt (qSDV) and the quadratic-Speed-Dependent Hard-Collision (qSDHC) profiles. Numerical tests successfully confirm the analytically derived fact that all these profiles can be expressed as combinations of complex Voigt probability functions. Based on a slightly improved version of the CPF subroutine [Humlicek. J Quant Spectrosc Radiat Transfer 1979;21:309] for the calculation of the complex probability function, we show that the pCqSDHC, qSDHC and qSDV profiles can be quickly calculated with an accuracy better than 10^{-4}.

1. Introduction

With the considerable improvement of diode-laser and Fourier transform spectroscopy techniques (e.g. [1–4]) in terms of both signal-to-noise and resolution, and the requirements for increasing precision of Earth observation projects [5–8], the use of the Voigt profile is getting obsolete. A more accurate reference isolated line-shape model is now crucially needed for the extraction of spectroscopic data from laboratory measurements, the subsequent feeding of spectroscopic databases and the analysis of atmospheric spectra. While it is now clear that a more refined line-shape model than the Voigt profile must be used [9], the question "which one?" remained opened. Indeed, the different non-Voigt profiles used to fit experimental spectra are still highly disparate and probably chosen on an ad-hoc basis (as discussed in the introduction of Ref. [10]). It is thus important to find a consensus for the proper reference line-shape model. As mentioned in [10], this profile must fulfill the five following crucial criteria: (i) It should be sufficiently physically based and robust to represent the observed shapes of lines of many different molecules to better than a few 0.1%. (ii) It should involve well-identified and physically-meaningful line-by-line parameters with known dependences on the gas pressure (and temperature) in order to enable their storage in databases. (iii) Its practical computation should require a computer time compatible with the treatment, in radiative transfer codes, of thousands of optical transitions in various atmospheric layers. (iv) It should contain, as limit cases, as many of the previously used ones as possible, in order to maximize the possibility to use published results. (v) It should be compatible with a modeling of line-mixing effects.

In the companion paper [10], we have shown that the partially-Correlated quadratic-Speed-Dependent Hard-Collision (pCqSDHC) profile [11,12] offers a good compromise and fulfills these five requirements. It takes into account the different contributions to the non-Voigt line shape with well-identified line-by-line parameters: the collision-induced velocity-changes effects; the speed dependence of the broadening and shifting coefficients; the correlation between velocity and internal-states changes. Its limiting cases correspond to different existing models, making the use of many published results straightforward. Furthermore, it can be easily extended in order to take into

* Corresponding author. Tel.: +33 145176558.
E-mail address: ha.tran@lisa.u-pec.fr (H. Tran).

0022-4073/$ - see front matter © 2013 Elsevier Ltd. All rights reserved.
http://dx.doi.org/10.1016/j.jqsrt.2013.06.015

account line-mixing effects. Last but not least, we have shown that this profile can be written as combinations of complex probability functions and hence can be quickly calculated.

In this paper, FORTRAN subroutines for the calculation of this pCqSDHC model and of its two limits: the quadratic-Speed-Dependent Voigt (qSDV) and quadratic-Speed-Dependent Hard-Collision (qSDHC) profiles are provided. The line-shape expression is recalled in Section 2 of this paper and some of its asymptotic limits are presented in Section 3. The accuracy and the CPU speed of the pCqSDHC profile calculated as combinations of complex probability functions are discussed in Section 4 while some conclusions are drawn in Section 5.

2. Expression of the spectral profile

Within the partially-Correlated Speed-Dependent Hard-Collision model, the spectral profile of an isolated line is given by [10–12]:

$$I(\omega)=\frac{1}{\pi}\mathrm{Re}\left\{\frac{\int \mathrm{d}\vec{v} f_{\mathrm{MB}}(\vec{v})/[i(\omega-\omega_0-\vec{k}.\vec{v}-\Delta(v))+\Gamma(v)+\tilde{\nu}_{VC}(v)]}{1-\int \mathrm{d}\vec{v}\,\tilde{\nu}_{VC}(v) f_{\mathrm{MB}}(\vec{v})/[i(\omega-\omega_0-\vec{k}.\vec{v}-\Delta(v))+\Gamma(v)+\tilde{\nu}_{VC}(v)]}\right\}, \tag{1}$$

where ω_0 is the unperturbed angular frequency of the optical transition and $f_{\mathrm{MB}}(\vec{v})$ is the Maxwell–Boltzmann distribution, $\Gamma(v)$ and $\Delta(v)$ are the speed-dependent collisional width and shift while $\vec{k}.\vec{v}=(\omega_0/c)\vec{z}.\vec{v}$ is due to Doppler effect. $\tilde{\nu}_{VC}(v)$ is the speed-dependent velocity-changing collision frequency, given by [13,14]:

$$\tilde{\nu}_{VC}(v)=\nu_{VC}-\eta\{\Gamma(v)-i\Delta(v)\}, \tag{2}$$

with η the correlation parameter and ν_{VC} the frequency of velocity-changing collisions when assuming no correlation between velocity and rotational-state changes. Using quadratic dependences [15,16] of the line width and shift on the speed v, i.e.:

$$\begin{aligned}\Gamma(v)-i\Delta(v)&=(\Gamma_0-i\Delta_0)+(\Gamma_2-i\Delta_2)\left\{\left(\frac{v}{\tilde{v}}\right)^2-\frac{3}{2}\right\}\\&=C_0+C_2\left\{\left(\frac{v}{\tilde{v}}\right)^2-\frac{3}{2}\right\},\end{aligned} \tag{3}$$

the line-shape can be written as [10]:

$$I^{\mathrm{pCqSDHC}}(\omega)=\frac{1}{\pi}\mathrm{Re}\left\{\frac{A(\omega)}{1-[\nu_{VC}-\eta(C_0-3C_2/2)]A(\omega)+(\eta C_2/\tilde{v}^2)B(\omega)}\right\}. \tag{4}$$

The $A(\omega)$ and $B(\omega)$ terms can be expressed as combination of the complex probability function $w(z)$:

$$\begin{aligned}\frac{1}{\pi}A(\omega)&=\frac{c}{\sqrt{\pi}\omega_0\tilde{v}}[w(iZ_1)-w(iZ_2)],\\B(\omega)&=\frac{\tilde{v}^2}{\tilde{C}_2}\left[-1+\frac{\sqrt{\pi}}{2\sqrt{Y}}(1-Z_1^2)w(iZ_1)-\frac{\sqrt{\pi}}{2\sqrt{Y}}(1-Z_2^2)w(iZ_2)\right],\end{aligned} \tag{5}$$

with $w(z)$ given by [17]:

$$w(z)=\frac{i}{\pi}\int_{-\infty}^{+\infty}\frac{e^{-t^2}dt}{z-t}=e^{-z^2}erfc(-iz), \tag{6}$$

and

$$\begin{aligned}Z_1&=\sqrt{X+Y}-\sqrt{Y}\\&=\sqrt{\left[i(\omega-\omega_0)+\tilde{C}_0\right]/\tilde{C}_2+\left(\frac{\omega_0\tilde{v}}{2c\tilde{C}_2}\right)^2}-\frac{\omega_0\tilde{v}}{2c\tilde{C}_2},\\Z_2&=\sqrt{X+Y}+\sqrt{Y}\\&=\sqrt{\left[i(\omega-\omega_0)+\tilde{C}_0\right]/\tilde{C}_2+\left(\frac{\omega_0\tilde{v}}{2c\tilde{C}_2}\right)^2}+\frac{\omega_0\tilde{v}}{2c\tilde{C}_2},\end{aligned} \tag{7}$$

where

$$X=\left[i(\omega-\omega_0)+\tilde{C}_0\right]/\tilde{C}_2 \text{ and } Y=\left(\frac{\omega_0\tilde{v}}{2c\tilde{C}_2}\right)^2 \tag{8}$$

In Eqs. (4)–(8), $\tilde{C}_0=(1-\eta)(C_0-3C_2/2)+\nu_{VC}$ and $\tilde{C}_2=(1-\eta)C_2$, $\tilde{v}$ is the most probable speed $\tilde{v}=\sqrt{2k_BT/m}$ with m the molecular mass, so that one has the relation $\frac{\omega_0\tilde{v}}{c}=\frac{\Gamma_D}{\sqrt{\ln 2}}$ with Γ_D the Doppler width.

Numerous efficient Fortran softwares are available for the calculation of $w(z)$ function (e.g. [18–23]). Using the CPF subroutine proposed by Humlicek [18] and slightly improved,[1] a FORTRAN subroutine has been built in order to calculate the spectral profile $I(\omega)$ of the pCqSDHC model. Furthermore, FORTRAN subroutines for simpler profiles, corresponding to different limits of the pCqSDHC model: the qSDV [i.e. $\eta=0$ and $\nu_{VC}=0$ in Eqs. (2)–(7)]; the qSDHC [i.e. $\eta=0$ in Eqs. (2)–(7)] are also provided. These FORTRAN subroutines are provided as supplementary material associated to this paper and also available upon request to the corresponding author.

3. Some asymptotic limits

The pCqSDVP profile as written in Eqs. (4)–(7), involves some differences [e.g. in the definitions of $A(\omega)$ and Z_1] which may be poorly calculated, due to the limited computer precision, when the two terms involved have very close values. Furthermore, problems may be encountered if some parameters are zero (e.g. if there is no speed dependence and $|\tilde{C}_2|=0$). In order to avoid such problems, various asymptotic limits have been derived, which are used in the FORTRAN routines and are described below.

3.1. When $|\tilde{C}_2|$ tends toward zero

A first limit to be considered is when $|\tilde{C}_2|$ tends toward zero [e.g. $\eta\to 1$ or/and $(\Gamma_2-i\Delta_2)\to 0$]. In this case, a first order development of Eq. (7) gives:

$$Z_1\to\frac{i(\omega-\omega_0)+\tilde{C}_0}{\Gamma_D/\sqrt{\ln 2}} \text{ and } Z_2=2\sqrt{Y}+Z_1\to\frac{\Gamma_D}{\sqrt{\ln 2}\tilde{C}_2}\to+\infty, \tag{9}$$

[1] A new region for large values of z [see Eq. (6)] has been added in the CPF subroutine.

the corresponding $A(\omega)$ and $B(\omega)$ terms in Eq. (5) thus become:

$$\begin{aligned}&\tfrac{1}{\pi}A(\omega)\rightarrow\tfrac{\sqrt{\ln 2}}{\sqrt{\pi}\Gamma_D}w(iZ_1),\\&B(\omega)\rightarrow\tfrac{\sqrt{\pi}\tilde{\nu}^2\sqrt{\ln 2}}{\Gamma_D}\left[(1-Z_1^2)w(iZ_1)+\tfrac{Z_1}{\sqrt{\pi}}\right],\\&\text{and } B(\omega)\rightarrow\tfrac{\sqrt{\pi}\tilde{\nu}^2\sqrt{\ln 2}}{\Gamma_D}\left[w(iZ_1)+\tfrac{1}{2\sqrt{\pi}Z_1}-\tfrac{3}{4\sqrt{\pi}Z_1^3}\right]\text{ when }|Z_1|\rightarrow\infty.\end{aligned}\tag{10}$$

3.2. When $|Y|$ is much larger than $|X|$ (i.e. $|X|/|Y|\rightarrow 0$)

A second limit must be derived when $|X|/|Y|\rightarrow 0$ since Z_1 becomes the difference of two nearly equal terms (i.e. $\sqrt{X+Y}\rightarrow\sqrt{Y}$). Its value may thus be incorrectly calculated due to the limited precision of computers. In this case, Z_1 can be replaced by its first order development $Z_1\rightarrow\{i(\omega-\omega_0)+\tilde{C}_0\}/(\Gamma_D/\sqrt{\ln 2})$.

3.3. When $|Y|$ is much smaller than $|X|$ (i.e. $|Y|/|X|\rightarrow 0$)

Finally, when $|Y|/|X|\rightarrow 0$ (when Γ_D approaches 0 for example), Z_1 and Z_2 become very close to each other. Again, the limited precision of computers may then induce large relative errors in the evaluations of the differences $[w(iZ_1)-w(iZ_2)]$ and $[Z_1^2w(iZ_1)-Z_2^2w(iZ_2)]$ appearing in the $A(\omega)$ and $B(\omega)$ terms [Eq. (5)]. In this case, $A(\omega)$ and $B(\omega)$ can be straightforwardly written as:

$$\begin{aligned}&\tfrac{1}{\pi}A(\omega)\rightarrow\tfrac{2}{\sqrt{\pi}\tilde{C}_2}\left[\tfrac{1}{\sqrt{\pi}}-\sqrt{X}w(i\sqrt{X})\right],\\&B(\omega)\rightarrow\tfrac{\tilde{\nu}^2}{\tilde{C}_2}\left[-1+2\sqrt{\pi}(1-X-2Y)\left\{\tfrac{1}{\sqrt{\pi}}-\sqrt{X}w(i\sqrt{X})\right\}\right.\\&\qquad\left.+2\sqrt{\pi}\sqrt{X+Y}w(i\sqrt{X+Y})\right].\end{aligned}\tag{11}$$

Note that the $\sqrt{X}w(i\sqrt{X})$ term in Eq. (11) tends toward $1/\sqrt{\pi}$ when $|\sqrt{X}|\rightarrow\infty$. In this case, Eq. (11) becomes:

$$\begin{aligned}&\tfrac{1}{\pi}A(\omega)\rightarrow\tfrac{1}{\pi\tilde{C}_2}\left[\tfrac{1}{X}-\tfrac{3}{2X^2}\right],\\&B(\omega)\rightarrow\frac{\tilde{\nu}^2}{\tilde{C}_2}\left[-1+(1-X-2Y)\left[\frac{1}{X}-\frac{3}{2X^2}\right]\right.\\&\qquad\left.+2\sqrt{\pi}\sqrt{X+Y}w(i\sqrt{X+Y})\right].\end{aligned}\tag{12}$$

In order to determine below or above which values of $|X|/|Y|$ and $|\sqrt{X}|$ the above limits can be used (for a chosen precision requirement), spectra calculated by these equations and Eq. (4) have been compared with calculated reference spectra obtained from Eq. (1) by direct numerical integrations over the velocity $\vec{v}$. The results are discussed in Section 4 and included in the FORTRAN subroutines given in the Supplementary data.

4. Results and discussions

4.1. Accuracy

The comparisons between spectra calculated with the pCqSDHC written as combination of complex probability functions [Eqs. (4) and (5)] and the various asymptotic limits (Section 3) and the calculated reference spectra computed from Eq. (1) by direct numerical integrations over $\vec{v}$ have been made. That was done for numerous sets of the spectral profile parameters (i.e. Γ_D, Γ_0, Γ_2, Δ_0, Δ_2, ν_{VC}, η and $\omega-\omega_0$) by varying each of them in broad ranges (i.e. $10^{-7}\leq\Gamma_D\leq10^{-2}$; $0.1\leq\Gamma_0/\Gamma_D\leq100$; $0\leq\Gamma_2/\Gamma_0\leq0.5$; $0\leq\Delta_0/\Gamma_0\leq10^{-2}$; $0\leq\Delta_2/\Delta_0\leq10^{-2}$; $0\leq\nu_{VC}/\Gamma_0\leq0.5$; $0\leq\eta\leq1$; $-10\Gamma_V\leq\omega-\omega_0\leq10\Gamma_V$ with Γ_V the corresponding estimated Voigt width [24]) thus leading to large ranges of the X and Y parameters in Eq. (8). For this exercise, two kinds of tests have been made. For the first one, the relevant complex Voigt probability functions [Eq. (6)] have been calculated by using numerical integration and for the second one, the CPF subroutine of Ref. [18] (slightly improved) was used. Note that, although the latter may not be the most precise nor optimized one available, comparison of different subroutines for the complex Voigt probability function is beyond the scope of this paper. We thus leave to the user the choice to change from the proposed CPF to another one.

The comparisons between the different calculations are shown in Fig. 1 where the maximum relative error for each spectrum [i.e. $\max(|A_{cal}-A_{ref}|)/A_{ref}$, with A_{cal} the absorption calculated following Eqs. (4)–(7) and Section 3 and A_{ref} the calculated reference absorption] is displayed. One can first see that the relative differences between calculated reference spectra and those calculated as combination of complex probability functions, are smaller than 10^{-9} when all integrals are calculated numerically. Since the analysis shows that these differences are entirely due to the limited computer precision, this confirms the validity of Eqs. (4)–(7) and of the different asymptotic limits. As expected, using the CPF subroutine [18] to calculate the complex probability function leads to larger relative errors, up to 10^{-4} due to the approximate nature of the rational expressions proposed in [18]. This error could obviously be reduced by using more precise subroutines but it remains sufficiently small for all current practical applications. Note that someone wishing to use a subroutine other than CPF should be very careful. Indeed, available subroutines often calculate the complex probability function in different regions (e.g. [18,21,22]) and the line-shape is related to the difference of two complex probability functions [Eq. (5)]. When these functions are close to each other but correspond to two different regions of the used subroutine, a large relative error can be obtained in the final result even if each of the two functions is accurately calculated. These possible amplifications of errors need to be studied carefully.

4.2. Speed

The maximum ratios of the computer time needed for the calculation of the pCqSDHC, qSDHC and qSDV profiles to that for the Voigt profile, using the CPF subroutine of Ref. [18], are given in Table 1. Three regions being considered in the CPF subroutine (see Supplementary data) which involve different computer times, the most time-consuming region (region II) needs about 2.5 times longer than the less time-consuming one (region I). Using this result and the formulation [Eqs. (4)–(12)] of the pCqSDHC profile as well as of the qSDHC and qSDV profiles, the maximum ratios of the computer time needed for the calculation of these profiles to that for the Voigt profile can be deduced. For example, in order to calculate

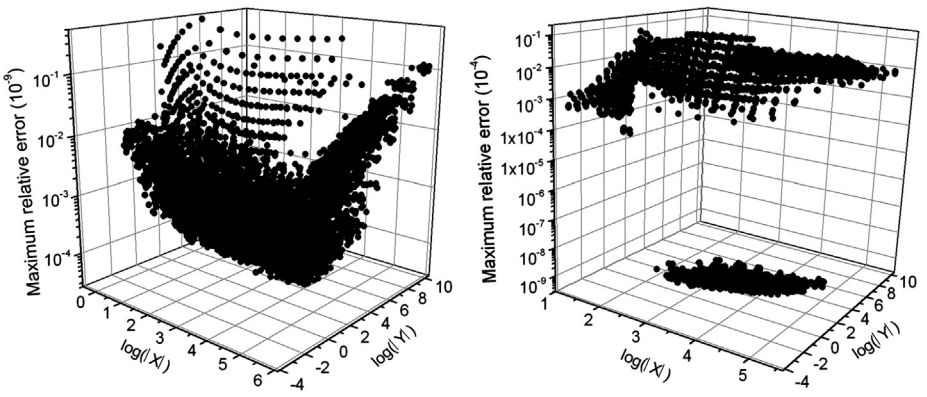

Fig. 1. Maximum relative differences between spectra calculated by direct numerical integrals through Eq. (1) and those calculated as a combination of complex probability functions [Eqs. (4)–(7) and Section 3] for all considered values of Γ_D, Γ_0, Γ_2, Δ_0, Δ_2, ν_{VC}, η. The left and right panels display the result obtained when $w(z)$ is computed by direct numerical integration of Eq. (6) and by using the CPF subroutine [18], respectively. The results are displayed versus the |X| and |Y| parameters [see Eq. (8)].

Table 1
Maximum ratios of the computer time needed for the calculation of the pCqSDHC, qSDHC and qSDV profiles to that for the Voigt profile.

Model	General case	Asymptotic limits		
		$\tilde{C}_2 = 0$	$\|X\|/\|Y\| \leq 3 \times 10^{-8}$	$\|Y\|/\|X\| \leq 10^{-15}$
pCqSDHC	5	2.5	5	5
qSDHC	5	2.5	5	2.5
qSDV	5	2.5	5	2.5

the pCqSDHC profile using Eqs. (4)–(7), one needs to call two times the CPF function, the maximum ratio of the computer time needed for this calculation to that for the corresponding Voigt profile can thus reach $2 \times 2.5 = 5$, the computer time for the calculation of different parameters being negligible compared to that for the CPF function. The values obtained for the three profiles are presented in Table 1. Note that ratios estimated in this way largely overestimate the value that would be obtained in a realistic spectral profile computation. Indeed, calculations made for the H_2O and CO_2 lines considered in Figs. 3 and 5 of Ref. [10] lead to a mean ratio of about 2–3.

Finally, note that the higher and lower limits for the application of the various asymptotic limits have been chosen based on the use of the CPF subroutine [18], they should thus be tested and then changed if necessary when another configuration is used.

5. Conclusion

The pCqSDHC model for an isolated line-shape presents a very good compromise between accuracy and computation efficiency. Its line-by-line structure with well-identified parameters allows an easy inclusion of this model in spectroscopic database and in radiative transfer calculations. It can be expressed as combination of complex probability functions and thus can be easily calculated. This previously analytically obtained result is confirmed in this paper by numerical tests. Based on a slightly improved version of the CPF subroutine [18] for the calculation of the complex probability function, we show that the pCqSDHC, qSDHC and qSDV profiles can be quickly calculated with an accuracy better than 10^{-4}. Corresponding FORTRAN subroutines for the calculation of these three models are provided. Note that the provided softwares are all written in complex, so that the inclusion of line-mixing effects by using the first-order approximation [25] through Eq. (9) of Ref. [10] is straightforward.

Appendix A. Supporting information

Supplementary data associated with this article can be found in the online version at http://dx.doi.org/10.1016/j.jqsrt.2013.06.015.

References

[1] Predoi-Cross A, Hambrook K, Keller R, Povey C, Schofield I, Hurtmans D, et al. Spectroscopic lineshape study of the self-perturbed oxygen A-band. J Mol Spectrosc 2008;248:85–110.
[2] Devi VM, Benner DC, Miller CE, Predoi-Cross A. Lorentz half-width, pressure-induced shift and speed-dependent coefficients in oxygen-broadened CO_2 bands at 6227 and 6348 cm^{-1} using a constrained multispectrum analysis. J Quant Spectrosc Radiat Transfer 2010;111:2355–69.
[3] DeVizia MD, Rohart F, Castrillo A, Fasci E, Moretti L, Gianfrani L. Speed-dependent effects in the near-infrared spectrum of self-colliding $H_2{}^{18}O$ molecules. Phys Rev A 2011;83:052506.
[4] Cygan A, Lisak D, Wojtewicz S, Domyslawska J, Hodges JT, Trawinski RS, et al. High-signal-to-noise-ratio laser technique for accurate measurements of spectral line parameters. Phys Rev A 2012;85:022508.
[5] Crisp D, Atlas RM, Breon F-M, Brown LR, Burrows JP, Ciais P, et al. The Orbiting Carbon Observatory (OCO) mission. Adv Space Res 2004;34:700–9.
[6] Miller CE, Brown LR, Toth RA, Benner DC, Devi VM. Spectroscopic challenges for high accuracy retrievals of atmospheric CO_2 and the Orbiting Carbon Observatory (OCO) experiment. C R Phys 2005;6:876–87.
[7] Miller CE, Crisp D, DeCola PL, Olsen SC, Randerson JT, Michalak AM, et al. Precision requirements for space-based data. J Geophys Res 2007;112:D10314. http://dx.doi.org/10.1029/2006JD007659.
[8] Thompson DR, Benner DC, Brown LR, Crisp D, Devi VM, Jiang Y, et al. Atmospheric validation of high accuracy CO_2 absorption coefficients for the OCO-2 mission. J Quant Spectrosc Radiat Transfer 2012;113:2265–76.
[9] Hartmann J-M, Boulet C, Robert D. Collisional effects on molecular spectra. Laboratory experiments and models, consequences for applications. Amsterdam: Elsevier; 2008.

[10] Ngo NH, Lisak D, Tran H, Hartmann J-M. An isolated line-shape model to go beyond the Voigt profile in spectroscopic databases and radiative transfer codes. J Quant Spectrosc Radiat Transfer, http://dx.doi.org/10.1016/j.jqsrt.2013.05.034, in press.
[11] Pine AS. Asymmetries and correlations in speed-dependent Dicke-narrowed line shapes of argon-broadened HF. J Quant Spectrosc Radiat Transfer 1999;62:397–423.
[12] Joubert P, Bonamy J, Robert D, Domenech J-L, Bermejo D. A partially correlated strong collision model for velocity- and state-changing collisions application to Ar-broadened HF rovibrational line shape. J Quant Spectrosc Radiat Transfer 1999;61:519–31.
[13] Rautian SG. Sobel'man II. The effect of collisions on the Doppler broadening of spectral lines. Sov Phys Usp 1967;9:701–16.
[14] Ngo NH, Tran H, Gamache RR. A pure H_2O isolated line-shape model based on classical molecular dynamics simulations of velocity changes and semi-classical calculations of speed-dependent collisional parameters. J Chem Phys 2012;136:154310.
[15] Rohart F, Mader H, Nicolaisen H-W. Speed dependence of rotational relaxation induced by foreign gas collisions: studies on CH_3F by millimeter wave coherent transients. J Chem Phys 1994;101:6475–86.
[16] Rohart F, Ellendt A, Kaghat F, Mäder H. Self and polar foreign gas line broadening and frequency shifting of CH3F: effect of the speed dependence observed by millimeter-wave coherent transients. J Mol Spectrosc 1997;185:222–33.
[17] Abramowitz M, Stegun IA. Handbook of mathematical functions with formulas, graphs, and mathematical tables. New York: Dover Publications; 1972.
[18] Humlicek J. An efficient method for evaluation of the complex probability function: the Voigt function and its derivatives. J Quant Spectrosc Radiat Transfer 1979;21:309–13.
[19] Schreier F. The Voigt and complex error function: a comparison of computational methods. J Quant Spectrosc Radiat Transfer 1992;48:743–62.
[20] Kuntz M. A new implementation of the Humlicek algorithm for the calculation of the Voigt profile function. J Quant Spectrosc Radiat Transfer 1997;57:819–24.
[21] Wells RJ. Rapid approximation to the Voigt/Faddeeva function and its derivatives. J Quant Spectrosc Radiat Transfer 1999;62:29–48.
[22] Letchworth KL, Benner DC. Rapid and accurate calculation of the Voigt function. J Quant Spectrosc Radiat Transfer 2007;107:173–92.
[23] Schreier F. Optimized implementations of rational approximations for the Voigt and complex error function. J Quant Spectrosc Radiat Transfer 2011;112:1010–25.
[24] Olivero JJ, Longbothum RL. Empirical fits to the Voigt line width: a brief review. J Quant Spectrosc Radiat Transfer 1977;17:233–6.
[25] Rosenkranz P. Shape of the 5 mm oxygen band in the atmosphere. IEEE Trans Antennas Propag 1975;23:498–506.